PERGAMON

Available online at www.sciencedirect.com

SCIENCE DIRECT®

Polyhedron 22 (2003) 1009–1018

POLYHEDRON

www.elsevier.com/locate/poly

Dioxovanadium(V) Schiff base complexes of *N*-methyl-1,2-diaminoethane and 2-methyl-1,2-diaminopropane with aromatic *o*-hydroxyaldehydes and *o*-hydroxyketones: synthesis, characterisation, catalytic properties and structure

Edmund Kwiatkowski [a,*], Grzegorz Romanowski [a], Waldemar Nowicki [a], Marek Kwiatkowski [a], Kinga Suwińska [b]

[a] *Department of Chemistry, University of Gdańsk, Sobieskiego 18, 80-952 Gdańsk, Poland*
[b] *Institute of Physical Chemistry, Polish Academy of Sciences, Kasprzaka 44/52, PL-01224 Warsaw, Poland*

Received 15 November 2002; accepted 20 January 2003

Abstract

Nineteen new dioxovanadium(V) complexes with unsymmetrical tridentate Schiff base ligands, obtained by a single condensation of 2-methyl-1,2-diaminopropane or *N*-methyl-1,2-diaminoethane with salicylaldehyde and its derivatives, 2-hydroxy-1-naphthaldehyde, 2-hydroxyacetophenone, 1-hydroxy-2-acetonaphthone and 2-hydroxybenzophenone, were prepared. The complexes were characterized by their ^{1}H and ^{51}V NMR, IR, and UV–Vis spectra. Crystal structure of the 2-(4-amino-4-methyl-2-aza-1-penten-1-yl-κ^2N)-3,5-dimethoxyphenolato-κO-dioxovanadium(V), $VO_2(C_{13}H_{19}N_2O_3)$, has been obtained by X-ray diffraction studies. The structure revealed a rarely encountered in VO_2(tridentate Schiff base) complexes a distorted trigonal-bipyramidal coordination geometry. The complexes comprising ligands derived either from *N*-methyl-1,2-diaminoethane or 2-methyl-1,2-diaminopropane and 5-methoxysalicylaldehyde catalyse the oxidation of thioanisole to the corresponding sulfoxide by cumene hydroperoxide.

Keywords: Complexes; Vanadium; Schiff bases

1. Introduction

Vanadium is a bioelement involved in various catalytic (haloperoxidases, nitrogenases) and inhibitory (e.g. towards phosphatases) processes [1,2]. Some of the vanadium compounds stimulate glucose uptake and inhibit lipid breakdown in a manner remarkably reminiscent of insulin effects [3]. Vanadium containing haloperoxidases catalyse the oxidation of halides in the presence of hydrogen peroxide to highly reactive intermediate, a hypohalous acid, which may react either with suitable nucleophilic acceptor, if present, forming a halogenated compound [4,5] or with hydrogen peroxide yielding $^{1}O_2$ [5,6]. Recently, it has been established that vanadium peroxidases are able to catalyse the oxidation of organic sulfides to the corresponding sulfoxides in the presence of hydrogen peroxide [7–10]. Messerschmidt et al. [11] showed by X-ray diffraction studies that the coordination geometry about vanadium in native chloroperoxidase from the fungus *Curvularia inaequalis* and its peroxide form is trigonal-bipyramidal (TBP) and distorted square-pyramidal, respectively. A deeper understanding of catalytic functions of vanadium peroxidases prompted for the synthesis and investigation of small-molecule models for active sites of these enzymes. A collection of such models discussed in some detail in a recent review [12] show that they contained either N_2O_2 or NO_{4-5} set of donor atoms in the coordination sphere. However the TBP coordination geometry in these compounds remains relatively rare. The examples of that geometry in vanadium(V) complexes are the [*N*-(3-methyl-6-*tert*-butylsalicylidene)-*N*′-methylethylenediaminato]dioxovanadium(V) [13], and the dioxovana-

* Corresponding author. Fax: +48-58-341-0357.
E-mail address: kwiat@chem.univ.gda.pl (E. Kwiatkowski).

0277-5387/03/$ - see front matter
doi:10.1016/S0277-5387(03)00041-X

dium(V) 1-[*N*-(quinolin-8-yl)]-naphthylaldimin-2-olate [14]. A scarcity of V(V) TBP complexes and their potent biological functions provide impetus for the synthesis and characterisation of new V(V) complexes. The present paper deals with the preparation of a group of compounds related to the complexes obtained by Mokry and Carrano [13] as well as new vanadium complexes comprising coordinated single condensation products of 2-methyl-1,2-diaminopropane and aromatic *o*-hydroxyaldehydes and *o*-hydroxyketones presented in Fig. 1, and with the characterisation of their spectroscopic (^{1}H, ^{51}V NMR, UV–Vis, IR) and catalytic properties in the reaction of oxidation of methyl phenyl sulfide to methyl phenyl sulfoxide by cumene hydroperoxide [15–17]. Crystal and molecular structure of 2-(4-amino-4-methyl-2-aza-1-penten-1-yl-κ^{2}N-3,5-dimethoxyphenolato-κO-dioxovanadium(V) is also reported.

2. Experimental

2.1. Measurements

Carbon, hydrogen and nitrogen contents were determined on a Carlo Erba MOD 1106 elemental analyser. FT-IR spectra of solid samples (KBr pellets) were run on a Bruker IFS 66, and electronic spectra on the Perkin–Elmer LAMBDA 18 spectrophotometer. ^{1}H and ^{51}V NMR spectra were obtained in DMSO-d_6 solutions at 50 °C with a Varian Mercury-400BB (400 MHz) spectrometer using TMS (^{1}H) and $VOCl_3$ (^{51}V) as reference compounds. Chromatography was carried out with a Hewlett-Packard 1050 chromatograph.

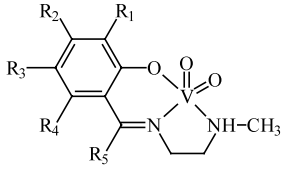

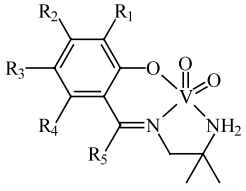

	R_1	R_2	R_3	R_4	R_5
1	H	H	H	H	H
2	H	H	OCH_3	H	H
3	H	H	CH_3	H	H
4	H	H	Br	H	H
5	H	H	NO_2	H	H
6	H	H	H	H	CH_3
7	H	H	H	H	C_6H_5
8	H	H	-$(CH)_4$-		H
9	-$(CH)_4$-		H	H	CH_3
10	H	OCH_3	H	OCH_3	H

	R_1	R_2	R_3	R_4	R_5
11	H	H	H	H	H
12	H	H	OCH_3	H	H
13	H	H	CH_3	H	H
14	H	H	Br	H	H
15	H	H	NO_2	H	H
16	H	H	H	H	CH_3
17	H	H	H	H	C_6H_5
18	H	H	-$(CH)_4$-		H
19	-$(CH)_4$-		H	H	CH_3
20	H	OCH_3	H	OCH_3	H

Fig. 1. Structural formulae of dioxovanadium(V) Schiff base complexes.

2.2. X-ray investigations

The structure of **20** was determined. Crystal data and refinement details are provided in Table 1. Data for the **20** complex were obtained with Mo Kα radiation using the Nonius–Kappa CCD diffractometer. Structure was solved using direct methods with SHELXS-97 [18] and refined by full-matrix least-squares using the SHELXL-97 [19] with anisotropic thermal parameters for the non-hydrogen atoms. Hydrogen atoms on the carbon and nitrogen atoms were included in calculated positions and given thermal parameters equivalent to 1.2 times those of the atom to which they were attached. Selected bond lengths and angles are listed in Table 2.

2.3. Catalytic oxidation of sulfides

A DMSO solution of dioxovanadium(V) Schiff base complex (4×10^{-5} mol) was stirred with cumene hydroperoxide (4×10^{-3} mol) in DMSO (10 ml) for 5 h at 20 °C. To the resulting yellow solution heated to 50 °C the methyl phenyl sulfide (4×10^{-4} mol) dissolved in DMSO was added. The mixture was kept at 50 °C. The rate of the oxidation reaction was studied with the help of high performance liquid chromatography. Samples of the reaction mixture were withdrawn at intervals and then chromatographed with a Kromasil-

Table 1
Crystal data and structure refinement for **20**

Empirical formula	$C_{13}H_{19}N_2O_5V$
Formula weight	334.24
Temperature (K)	293(2)
Wavelength (Å)	0.71073
Crystal system	monoclinic
Space group	$P2_1/c$
Unit cell dimensions	
a (Å)	7.2840(2)
b (Å)	17.4510(5)
c (Å)	11.9370(3)
β (°)?	93.720(1)
Volume (Å^3)	1514.15(7)
Z	4
D_{calc} (g cm^{-3})	1.466
Absorption coefficient (mm^{-1})	0.677
$F(000)$	696
Crystal size (mm)	0.30 × 0.20 × 0.05
θ Range for data collection (°)	3.04–27.48
Limiting indices	$-9 \le h \le 9$, $-21 \le k \le 22$, $-15 \le l \le 15$
Reflections collected/unique	6434/3446 [$R_{int} = 0.021$]
Completeness to $\theta = 27.48$	99.1%
Refinement method	full-matrix least-squares on F^2
Data/restraints/parameters	3446/0/201
Final R indices [$I > 2\sigma(I)$]	$R_1 = 0.0383$, $wR_2 = 0.0881$
R indices (all data)	$R_1 = 0.0599$, $wR_2 = 0.0944$
Goodness-of-fit on F^2	1.033
Largest difference peak and hole (e Å^{-3})	0.242 and −0.281

Table 2
Selected bond lengths and angles (Å, °) for **20**

Bond lengths	
V1–O3	1.6252(14)
V1–O4	1.6181(14)
V1–O5	1.9064(13)
V1–N2	2.1085(17)
V1–N6	2.1257(17)
Bond angles	
O3–V1–O4	111.05(8)
O4–V1–O5	102.25(7)
O3–V1–O5	99.24(7)
O3–V1–N2	131.39(7)
O4–V1–N2	115.76(8)
O5–V1–N2	83.36(6)
O3–V1–N6	89.48(7)
O4–V1–N6	93.70(7)
O5–V1–N6	157.53(7)
N2–V1–N6	75.44(6)

100 C-8 column (Knauer GmBH, Germany) and acetonitrile–water (4:6 v/v) as an eluent. Chromatography was carried out with a flow rate of 1 ml min^{-1} and components were detected with spectrophotometric detector at 260 nm.

2.4. Complexes

Triethyl vanadate, $VO(OEt)_3$, and Schiff base complexes were prepared by methods analogous to the literature procedure of Root et al. [20]. Typically, 10 mmol of *N*-methyl-1,2-diaminoethane (MeNen) or 2-methyl-1,2-diaminopropane (Mepn) in 10 ml absolute EtOH was added with stirring to a freshly filtered solution of triethyl vanadate (10 mmol) in 250 ml of absolute EtOH producing a suspension of an intermediate. Then to the suspension was added slowly the desired aromatic *o*-hydroxyaldehyde (salicylaldehyde, 5-methoxysalicylaldehyde, 5-methylsalicylaldehyde, 5-bromosalicylaldehyde, 5-nitrosalicylaldehyde, 4,6-dimethoxysalicylaldehyde or 2-hydroxy-1-naphthaldehyde) or the aromatic *o*-hydroxyketone (2-hydroxyacetophenone, 1-hydroxy-2-acetonaphthone or 2-hydroxybenzophenone) in 10 ml of absolute EtOH. After refluxing and stirring for 2 (aldehydes) or 10 h (ketones) the separated yellow solids were filtered off, washed several times with absolute EtOH and Et_2O, and then dried. The complexes containing nitro and bromo substituents were recrystallized from DMSO–EtOH mixtures. Crystals suitable for X-ray analysis were obtained by slow crystallisation of purified **20** from DMSO.

2.4.1. 2-(2,5-Diaza-1-hexen-1-yl-κ^2N)-phenolato-κO-dioxovanadium(V) (**1**)

Yield 71%. *Anal.* Calc. for $C_{10}H_{13}N_2O_3V$: C, 46.2; H, 5.0; N, 10.8. Found: C, 46.2; H, 5.2; N, 10.8%. IR (KBr, cm^{-1}): 3233 (ν_{N-H}); 1641, 1598 ($\nu_{C=N}+\nu_{C=C}$); 927, 845 ($\nu_{V=O}$). Absorption spectrum in DMSO [λ_{max} (nm), ε (1 mol^{-1} cm^{-1})]: 369 (3740).

2.4.2. 2-(2,5-Diaza-1-hexen-1-yl-κ^2N)-4-methoxyphenolato-κO-dioxovanadium(V) (**2**)

Yield 80%. *Anal.* Calc. for $C_{11}H_{15}N_2O_4V$: C, 45.6; H, 5.2; N, 9.7. Found: C, 45.6; H, 5.3; N, 9.5%. IR (KBr, cm^{-1}): 3251 (ν_{N-H}): 1644, 1612 ($\nu_{C=N}+\nu_{C=C}$); 932, 847 ($\nu_{V=O}$). Absorption spectrum in DMSO [λ_{max} (nm), ε (1 mol^{-1} cm^{-1})]: 404 (3900).

2.4.3. 2-(2,5-Diaza-1-hexen-1-yl-κ^2N)-4-methylphenolato-κO-dioxovanadium(V) (**3**)

Yield 69%. *Anal*. Calc. for $C_{11}H_{15}N_2O_3V$: C, 48.2; H, 5.5; N, 10.2. Found: C, 48.0; H, 5.5; N, 10.0%. IR (KBr, cm^{-1}): 3232 (ν_{N-H}): 1633, 1591 ($\nu_{C=N}+\nu_{C=C}$); 924, 846 ($\nu_{V=O}$). Absorption spectrum in DMSO [λ_{max} (nm), ε (1 mol^{-1} cm^{-1})]: 384 (3520).

2.4.4. 2-(2,5-Diaza-1-hexen-1-yl-κ^2N)-4-bromophenolato-κO-dioxovanadium(V) (**4**)

Yield 75%. *Anal.* Calc. for $C_{10}H_{12}BrN_2O_3V$: C, 35.4; H, 3.6; N, 8.3. Found: C, 35.6; H, 3.6; N, 8.3%. IR (KBr, cm^{-1}): 3248 (ν_{N-H}); 1646, 1606 ($\nu_{C=N}+\nu_{C=C}$); 933, 849 ($\nu_{V=O}$). Absorption spectrum in DMSO [λ_{max} (nm), ε (1 mol^{-1} cm^{-1})]: 378 (3540).

2.4.5. 2-(2,5-Diaza-1-hexen-1-yl-κ^2N)-4-nitrophenolato-κO-dioxovanadium(V) (**5**)

Yield 83%. *Anal.* Calc. for $C_{10}H_{12}N_3O_5V$: C, 39.4; H, 4.0; N, 13.8. Found: C, 39.3; H, 4.1; N, 13.7%. IR (KBr, cm^{-1}): 3247 (ν_{N-H}); 1644, 1603 ($\nu_{C=N}+\nu_{C=C}$); 939, 845 ($\nu_{V=O}$). Absorption spectrum in DMSO [λ_{max} (nm), ε (1 mol^{-1} cm^{-1})]: 354 (17 600).

2.4.6. 2-(3,6-Diaza-2-hepten-1-yl-κ^2N)-phenolato-κO-dioxovanadium(V) (**6**)

Yield 77%. *Anal*. Calc. for $C_{11}H_{15}N_2O_3V$: C, 48.2; H, 5.5; N, 10.2. Found: C, 48.0; H, 5.5; N, 10.1%. IR (KBr, cm^{-1}): 3234 (ν_{N-H}); 1637, 1596 ($\nu_{C=N}+\nu_{C=C}$); 928, 841 ($\nu_{V=O}$). Absorption spectrum in DMSO [λ_{max} (nm), ε (1 mol^{-1} cm^{-1})]: 354 (3400).

2.4.7. 2-(1-Phenyl-2,5-Diaza-1-hexen-1-yl-κ^2N)-phenolato-κO-dioxovanadium(V) (**7**)

Yield 67%. *Anal.* Calc. for $C_{16}H_{17}N_2O_3V$: C, 57.1; H, 5.1; N, 8.3. Found: C, 57.0; H, 5.0; N, 8.2%. IR (KBr, cm^{-1}): 3218 (ν_{N-H}); 1639, 1602 ($\nu_{C=N}+\nu_{C=C}$); 932, 855 ($\nu_{V=O}$). Absorption spectrum in DMSO [λ_{max} (nm), ε (1 mol^{-1} cm^{-1})]: 371 (3540).

2.4.8. 1-(2,5-Diaza-1-hexen-1-yl-κ^2N)-2-naphtholato-κO-dioxovanadium(V) (**8**)

Yield 56%. *Anal.* Calc. for $C_{14}H_{15}N_2O_3V$: C, 54.2; H, 4.9; N, 9.0. Found: C, 54.1; H, 5.0; N, 8.9%. IR (KBr,

cm^{-1}): 3253 (ν_{N-H}); 1627, 1594 ($\nu_{C=N}+\nu_{C=C}$); 929, 855 ($\nu_{V=O}$). Absorption spectrum in DMSO [λ_{max} (nm), ε (1 mol^{-1} cm^{-1})]: ?322 (10 280), 397 (5940).

2.4.9. 2-(3,6-Diaza-1-hepten-1-yl-κ^2N)-1-naphtholato-κO-dioxovanadium(V) (**9**)

Yield 70%. *Anal.* Calc. for $C_{15}H_{17}N_2O_3V$: C, 55.6; H, 5.3; N, 8.6. Found: C, 55.6; H, 5.4; N, 8.7%. IR (KBr, cm^{-1}): 3246 (ν_{N-H}); 1621, 1590 ($\nu_{C=N}+\nu_{C=C}$); 937, 852 ($\nu_{V=O}$). Absorption spectrum in DMSO [λ_{max} (nm), ε (1 mol^{-1} cm^{-1})]: 326 (4960), 391 (5700).

2.4.10. 2-(2,5-Diaza-1-hexen-1-yl-κ^2N)-3,5-dimethoxyphenolato-κO-dioxovanadium(V) (**10**)

Yield 83%. *Anal.* Calc. for $C_{12}H_{17}N_2O_5V$: C, 45.0; H, 5.4; N, 8.7. Found: C, 45.2; H, 5.4; N, 8.7%. IR (KBr, cm^{-1}): 3226 (ν_{N-H}); 1630, 1600 ($\nu_{C=N}+\nu_{C=C}$); 932, 871($\nu_{V=O}$). Absorption spectrum in DMSO [λ_{max} (nm), ε (1 mol^{-1} cm^{-1})]: 319 (16 620).

2.4.11. 2-(4-Amino-4-methyl-2-aza-1-penten-1-yl-κ^2N)-phenolato-κO-dioxovanadium(V) (**11**)

Yield 90%. *Anal.* Calc. for $C_{11}H_{15}N_2O_3V$: C, 48.2; H, 5.5; N, 10.2. Found: C, 48.0; H, 5.6; N, 10.0%. IR (KBr, cm^{-1}): 3214, 3147 (ν_{N-H}); 1632, 1600 ($\nu_{C=N}+\nu_{C=C}$); 952, 877 ($\nu_{V=O}$). Absorption spectrum in DMSO [λ_{max} (nm), ε (1 mol^{-1} cm^{-1})]: 370 (3950).

2.4.12. 2-(4-Amino-4-methyl-2-aza-1-penten-1-yl-κ^2N)-4-methoxyphenolato-κO-dioxovanadium(V) hemiethanol solvate hemihydrate (**12**)

Yield 78%. *Anal.* Calc. for $C_{13}H_{21}N_2O_5V$: C, 46.4; H, 6.3; N, 8.3. Found: C, 46.6; H, 6.5; N, 8.1%. IR (KBr, cm^{-1}): 3383, 3258, 3225, 3142 ($\nu_{N-H}\nu_{OH}$); 1638, 1610 ($\nu_{C=N}+\nu_{C=C}$); 918, 850 ($\nu_{V=O}$). Absorption spectrum in DMSO [λ_{max} (nm), ε (1 mol^{-1} cm^{-1})]: 402 (3350).

2.4.13. 2-(4-Amino-4-methyl-2-aza-1-penten-1-yl-κ^2N)-4-methylphenolato-κO-dioxovanadium(V) (**13**)

Yield 68%. *Anal.* Calc. for $C_{12}H_{17}N_2O_3V$: C, 50.0; H, 5.9; N, 9.7. Found: C, 50.0; H, 6.2; N, 9.6%. IR (KBr, cm^{-1}): 3208, 3122 (ν_{N-H}); 1629, 1596 ($\nu_{C=N}+\nu_{C=C}$); 920, 952 ($\nu_{V=O}$). Absorption spectrum in DMSO [λ_{max} (nm), ε (1 mol^{-1} cm^{-1})]: 383 (3640).

2.4.14. 2-(4-Amino-4-methyl-2-aza-1-penten-1-yl-κ^2N)-4-bromophenolato-κO-dioxovanadium(V) (**14**)

Yield 59%. *Anal.* Calc. for $C_{11}H_{14}BrN_2O_3V$: C, 37.4; H, 4.0; N, 7.9. Found: C, 37.3; H, 3.9; N, 7.8%. IR (KBr, cm^{-1}): 3203, 3123 (ν_{N-H}); 1650, 1602 ($\nu_{C=N}+\nu_{C=C}$); 928, 846 ($\nu_{V=O}$). Absorption spectrum in DMSO [λ_{max} (nm), ε (1 mol^{-1} cm^{-1})]: 378 (3430).

2.4.15. 2-(4-Amino-4-methyl-2-aza-1-penten-1-yl-κ^2N)-4-nitrophenolato-κO-dioxovanadium(V) (**15**)

Yield 75%. *Anal.* Calc. for $C_{11}H_{14}N_3O_5V$: C, 41.4; H, 4.4; N, 13.2. Found: C, 41.2; H, 4.6; N, 13.1%. IR (KBr, cm^{-1}): 3190, 3116 (ν_{N-H}); 1653, 1606 ($\nu_{C=N}+\nu_{C=C}$); 928, 857 ($\nu_{V=O}$). Absorption spectrum in DMSO [λ_{max} (nm), ε (1 mol^{-1} cm^{-1})]: 353 (17 680).

2.4.16. 2-(5-Amino-5-methyl-3-aza-2-hexen-2-yl-κ^2N)-phenolato-κO-dioxovanadium(V) (**16**)

Yield 66%. *Anal.* Calc. for $C_{12}H_{17}N_2O_3V$: C, 50.0; H, 5.9; N, 9.7. Found: C, 50.0; H, 5.8; N, 9.8%. IR (KBr, cm^{-1}): 3191, 3128 (ν_{N-H}); 1633, 1595 ($\nu_{C=N}+\nu_{C=C}$); 912, 854 ($\nu_{V=O}$). Absorption spectrum in DMSO [λ_{max} (nm), ε (1 mol^{-1} cm^{-1})]: 349 (4070).

2.4.17. 2-(1-Phenyl-4-amino-4-methyl-2-aza-1-penten-1-yl-κ^2N)-phenolato-κO-dioxovanadium(V) (**17**)

Yield 77%. *Anal.* Calc. for $C_{17}H_{19}N_2O_3V$: C, 58.3; H, 5.5; N, 8.0. Found: C, 58.2; H, 5.3; N, 8.1%. IR (KBr, cm^{-1}): 3132, 3222 (ν_{N-H}); 1628, 1596 ($\nu_{C=N}+\nu_{C=C}$); 937, 852 ($\nu_{V=O}$). Absorption spectrum in DMSO [λ_{max} (nm), ε (1 mol^{-1} cm^{-1})]: 364 (4020).

2.4.18. 1-(4-Amino-4-methyl-2-aza-1-penten-1-yl-κ^2N)-2-naphtholato-κO-dioxovanadium(V) (**18**)

Yield 68%. *Anal.* Calc. for $C_{15}H_{17}N_2O_3V$: C, 55.6; H, 5.3; N, 8.6. Found: C, 55.7; H, 5.1; N, 8.5%. IR (KBr, cm^{-1}): 3282, 3223 (ν_{N-H}); 1622, 1596 ($\nu_{C=N}+\nu_{C=C}$); 926, 857 ($\nu_{V=O}$). Absorption spectrum in DMSO [λ_{max} (nm), ε (1 mol^{-1} cm^{-1})]: 322 (11 090), 394 (6430).

2.4.19. 2-(5-Amino-5-methyl-3-aza-2-hexen-2-yl-κ^2N)-1-naphtholato-κO-dioxovanadium(V) (**19**)

Yield 75%. *Anal.* Calc. for $C_{16}H_{19}N_2O_3V$: C, 56.8; H, 5.7; N, 8.3. Found: C, 57.0; H, 5.5; N, 8.3%. IR (KBr, cm^{-1}): 3250, 3191 (ν_{N-H}); 1620, 1592 ($\nu_{C=N}+\nu_{C=C}$); 946, 907 ($\nu_{V=O}$). Absorption spectrum in DMSO [λ_{max} (nm), ε (1 mol^{-1} cm^{-1})]: 327 (4830), 384 (4980).

2.4.20. 2-(4-Amino-4-methyl-2-aza-1-penten-1-yl-κ^2N)-3,5-dimethoxyphenolato-κO-dioxovanadium(V) (**20**)

Yield 57%. *Anal.* Calc. for $C_{13}H_{19}N_2O_5V$: C, 46.7; H, 5.7; N, 8.4. Found: C, 46.8; H, 5.6; N, 8.5%. IR (KBr, cm^{-1}): 3226, 3137 (ν_{N-H}); 1630, 1602 ($\nu_{C=N}+\nu_{C=C}$); 932, 871 ($\nu_{V=O}$). Absorption spectrum in DMSO [λ_{max} (nm), ε (1 mol^{-1} cm^{-1})]: 319 (18 570).

3. Results and discussion

The complexes presented in Fig. 1 were formed in a template reaction of equimolar amounts of an aromatic *o*-hydroxyaldehyde (or *o*-hydroxyketone) with *N*-methyl-1,2-diaminoethane or 2-methyl-1,2-diaminopropane and with triethyl vanadate in absolute ethanol solution.

The complexes are soluble in dipolar aprotic solvents but sparingly soluble in common organic solvents. IR spectra of solid complexes show strong bands at around 850 and 930 cm^{-1} which may be assigned to symmetric and asymmetric ν(O=V=O) vibration of the *cis*-VO_2 group. The spectrum shows moreover ν(C=N+C=C) vibrations in the range 1620–1653 for all the complexes and one and two ν(N–H) vibrations in the range 3150–3280 cm^{-1} for complexes derived from MeNen and Mepn, respectively; in the latter case they are assigned to antisymmetric and symmetric nitrogen–hydrogen stretching modes of primary amino group.

In the UV–Vis region the complexes show bands at approximately 325 nm and weaker bands in the range 349–404 nm. The weak bands were attributed to intramolecular charge transfer transitions [14] from the p_π orbital on the phenolate oxygen to the empty d orbitals of the metal. Positions of these ligand-to-metal charge transfer bands (l.m.c.t.) affect ring-substituents *trans* to the oxygen in complexes comprising 5X-salicylaldimino moiety indicating their significant influence on the energy of HOMO associated with the oxygen atom due to conjugative electronic effects between *para*-X and O atom. The l.m.c.t. energy of complexes derived from MeNen decreases in the order: $10 > 6 > 5 > 7 \sim 1 > 4 > 3 > 9 > 8 > 2$ and likely for analogous complexes derived from Mepn: $20 > 16 > 15 > 17 \sim 11 > 14 > 13 > 19 > 18 > 12$. The intense 319–327 nm bands were assigned to π–π* (intraligand) transitions [14].

The ^1H and ^{51}V NMR of the complexes were run in DMSO-d_6. The values of chemical shifts are reported in Table 3. ^1H NMR signals were assigned on the basis of intensity, spin–spin coupling patterns, chemical shift values and deuteration experiments. The ^1H NMR spectra of all complexes show the simultaneous occurrence of two sets of signals, which are attributable on one hand to the aromatic entities and on the other hand to the aliphatic moiety. Complex multiplets associated with protons of the aliphatic moiety of **1**–**10** complexes indicate the non-equivalence of all the methylene protons in the five-membered chelate ring and provide evidence for rigidity of the molecules in solution. All the methylene protons are non-equivalent or diastereotopic owing to their proximity to the chiral centre generated by the coordinated and unequally substituted secondary amino group. The high field signal of one of the methylene protons which appears as well resolved quartet of doublets at $\delta = 2.635$ ppm for **1**, collapses to triplet of doublets on exchange of the neighbouring NH proton for deuterium after addition of D_2O. Large difference in chemical shift of that methylene and the NH protons in comparison with the coupling constant allowed to use the first order spectra splitting diagram for estimation of the value of that constant ($^3J = 11.2$ Hz) and to conclude that these protons are antiperiplanar. The CH_2, NH_2, $C(CH_3)_2$ signals of **11**–**20** complexes appear as singlets corresponding to spin systems (A_2 or A_6) of chemically equivalent nuclei. The proximity of the methyl protons to the unsubstituted phenyl ring and their outside position of the ring plane in **17** results in an increase of their shielding ($\delta = 3.304$ ppm) relative to CH_2 protons in **11**–**16** and **18**–**20** ($\delta = 3.721$–3.920 ppm) due to the ring current effect. A decrease in shielding of the azomethine proton by going from **1** ($\delta = 8.900$ ppm) to **8** ($\delta = 9.758$ ppm) and from **11** ($\delta = 8.836$ ppm) to **18** ($\delta = 9.665$ ppm) equal on average to $\Delta\sigma = 0.835$ ppm, is associated with the ring current effect of single or two fused aromatic rings and shows that the aldimino hydrogen lies in the plane of these rings. Taking into account the additivity of contributions of individual aromatic rings to the ring current effect [21] we calculated the contribution of the unsubstituted fused naphthalene ring to that effect obtaining the value of $\Delta\sigma' = -0.741$ ppm on the basis of equation: $\Delta\sigma'|\text{ppm}| = -0.0276R^{-3}$ [21] and $R = 0.334$ nm, where the value of R is the separation of the azomethine proton from the centre of unsubstituted ring of naphthalene moiety. The $\Delta\sigma'$ differs not much from the experimental $\Delta\sigma$ value.

^{51}V NMR signals of complexes depend on the kind of amine used for the preparation of the complex but are independent on the aromatic part of the ligand. While the vanadium atom in complexes derived from Mepn absorbs in average at -550.3 ± 2.8 ppm, near to the range from -553 to -556 ppm reported for related VO_2L complexes [20], the resonances of vanadium in complexes derived from MeNen occur in average at -531.0 ± 4.4 ppm.

3.1. Crystal and molecular structure of *20*

The crystal structure consists of complex molecules (Fig. 2) linked by hydrogen bonding interactions. The geometry about vanadium is TBP considerably distorted. The degree of the distortion calculated on the basis of dihedral angle method [22] is 41.2% TBP–SP (SP = square pyramid). The singly deprotonated Schiff base ligand is coordinated meridionally occupying two apical positions one by O and the other by N(amino) atoms and one equatorial position by N(azomethine) atom. The two oxo groups occupy the remaining equatorial positions. Non-hydrogen atoms of the aromatic ring and its substituents [O5, O7, O8, N2, C9, C10, C11, C12, C13, C14, C15, C18, C19] are roughly in the plane (maximal deviation = 0.062 Å) with vanadium atom 0.610 Å out of that plane. Due to that latter deviation the conformation of the six-membered chelate ring [V1, O5, C9, C14, C15, N2] is concluded to be an envelope. Cremer and Pople [23] puckering analysis shows that the five-membered chelate ring containing V1, N2, C16, C17, N6 atoms adopts also an envelope

Table 3
Chemical shifts for protons of dioksovanadium(V) Schiff base complexes, **1**–**20**, in DMSO-d_6 (values of coupling constants are given in parentheses)

Compound	N–H	N–CH_3	N=CH	N–CH*a*H*b*	=N–CH*a*H*b*	Aromatic	Others	^{51}V NMR
1	s; 1H; 5.900	d; 3H; 2.713 (5.6)	s; 1H; 8.900	(a) qd; 1H; 2.635 (11.1; 5.2) (b) bd; 1H; 3.070	(a) tdd; 1H; 3.923 (11.2; 5.2; 1.6) (b) bd; 1H; 4.071	d; 1H; 6.790 (7.6) t; 1H; 6.815 (7.2) t; 1H; 7.445 (7.2) d; 1H; 7.542 (7.6)		−531.6
2	s; 1H; 5.671	d; 3H; 2.720 (5.8)	s; 1H; 8.863	(a) qd; 1H; 2.628 (10.8; 5.2) (b) bd; 1H; 3.071	(a) t; 1H; 3.918 (b) dt; 1H; 4.052	d; 1H; 6.744 (8) d; 1H; 7.093 (2.8) dd; 1H; 7.119 (5.6; 2.8)	s; 3H; 3.372 (OCH_3)	−530.8
3	s; 1H; 5.683	d; 3H; 2.717 (5.6)	s; 1H; 8.830	(a) qd; 1H; 2.635 (10.8; 4.8) (b) bd; 1H; 3.060	(a) dt; 1H; 3.931 (b) bd; 1H; 4.046	d; 1H; 6.701 (8) dd; 1H; 7.276 (8; 2) s; 1H; 7.315 (5.6; 2.8)	s; 3H; 2.257 (CH_3)	−531.0
4	s; 1H; 5.705	d; 3H; 2.715 (5.2)	s; 1H; 8.866	(a) qd; 1H; 2.663 (10.8; 5.2) (b) bd; 1H; 3.093	(a) dt; 1H; 3.977 (b) overlapped	d; 1H; 6.760 (9) dd; 1H; 7.528 (9; 3) d; 1H; 7.741 (3)		−531.5
5	s; 1H; 5.710	d; 3H; 2.712 (5.6)	s; 1H; 9.032	overlapped	(a) dt; 1H; 3.981 (b) bd; 1H; 4.090	d; 1H; 6.906 (9) dd; 1H; 8.228 (9; 3) d; 1H; 8.588 (3)		−528.7
6	s; 1H; 5.594	d; 3H; 2.648 (5.6)		(a) qd; 1H; 2.859 (10.8; 5.6) (b) bd; 1H; 3.146	(a) dq; 1H; 3.780 (17; 4) (b) dt; 1H; 4.016 (17; 4)	d; 1H; 6.733 (8) t; 1H; 6.788 (8) td; 1H; 7.368 (8; 1.6) dd; 1H; 7.785 (8; 1.6)	s; 3H; 2.619 (CH_3C=N)	−534.3
7	s; 1H; 5.645	d; 3H; 2.694 (6.0)		(a) overlapped (b) bd; 1H; 2.970	m; 2H; 3.413–3.550	td; 1H; 6.607 (8; 1.2) dd; 1H; 6.747 (8; 1.2) dd; 1H; 6.843 (8; 1.2) m; 3H; 7.357–7.400 m; 3H; 7.557–7.658		−534.5
8	s; 1H; 5.865	d; 3H; 2.730	s; 1H; 9.758	overlapped	(a) td; 1H; 4.062 (b) d; 1H; 4.290	d; 1H; 7.040 (8) t; 1H; 7.370 (7.2) t; 1H; 7.586 (6.8) d; 1H; 7.848 (8) d; 1H; 7.992 (8) d; 1H; 7.992 (8) d; 1H; 8.381 (8)		−529.0
9	s; 1H; 5.719	d; 3H; 2.671 (5.6)		(a) overlapped (b) m; 1H; 2.912–2.976	(a) m; 1H; 3.817–3.892 (b) dt; 1H; 4.071 (15; 4)	d; 1H; 7.240 (8) td; 1H; 7.466 (8; 1) td; 1H; 7.580 (8; 1) d; 1H; 7.788 (4) d; 1H; 7.800 (4) d; 1H; 8.281 (8)	s; 3H; 2.697 (CH_3C=N)	−529.8
10	s; 1H; 5.706	d; 3H; 2.679 (6.0)	s; 1H; 8.949	(a) qd; 1H; 2.615 (9.8; 5.0) (b) bd; 1H; 3.016	(a) m; 1H; 3.884–3.926 (b) bd; 1H; 4.029	d; 1H; 5.960 (2) d; 1H; 5.985 (2)	s; 3H; 3.778 s; 3H; 3.855 (OCH_3)	−528.9
	NH_2	$C(CH_3)_2$	N=CH		=N–CH_2	Aromatic	Others	^{51}V NMR

Table 3 (*Continued*)

Compound	N–H	$N-CH_3$	N=CH	N–CH*a*H*b*	=N–CH*a*H*b*	Aromatic	Others	^{51}V NMR
11	s; 2H; 5.030	s; 6H; 1.223	s; 1H; 8.836		s; 2H; 3.765	d; 1H; 6.783 (8) t; 1H; 6.809 (7.2) td; 1H; 7.445 (7.6; 1.6) dd; 1H; 7.538 (7.6; 1.6)		−551.4
12	s; 2H; 4.989	s; 6H; 1.214	s; 1H; 8.787		s; 2H; 3.750	d; 1H; 6.737 (9) dd; 1H; 7.095 (9; 3) d; 1H; 7.124 (3)	s; 3H; 3.741 (OCH_3) t; H; 1.066 dq; 1H; 3.454 t; H; 4.218 (C_2H_5OH)	−550.6
13	s; 2H; 4.996	s; 6H; 1.213	s; 1H; 8.759		s; 2H; 3.754	d; 1H; 6.695 (8) dd; 1H; 7.267 (8; 2) d; 1H; 7.301 (2)	s; 3H; 2.254 (CH_3)	−550.4
14	s; 2H; 5.079	s; 6H; 1.220	s; 1H; 8.811		s; 2H; 3.778	d; 1H; 6.756 (9) dd; 1H; 7.529 (9; 3) d; 1H; 7.734 (3)		−551.3
15	s; 2H; 5.205	s; 6H; 1.250	s; 1H; 9.035		s; 2H; 3.844	d; 1H; 6.919 (9) dd; 1H; 8.233 (9; 3) d; 1H; 8.598 (3)		−550.2
16	s; 2H; 5.005	s; 6H; 1.236			s; 2H; 3.668	d; 1H; 6.769 t; 1H; 6.795 t; 1H; 7.362 (7) d; 1H; 7.767 (8)	s; 3H; 2.592 ($CH_3C=N$)	−551.0
17	s; 2H; 5.083	s; 6H; 1.130			s; 2H; 3.304	t; 1H; 6.623 (7.6) dd; 1H; 6.724 (8; 2) d; 1H; 6.826 m; 2H; 7.283–7.303 td; 1H; 7.381 (8; 1.6) m; 3H; 7.555–7.647		−552.0
18	s; 2H; 5.083	s; 6H; 1.254	s; 1H; 9.665		s; 2H; 3.940	d; 1H; 7.039 (9) t; 1H; 7.364 (7.6) td; 1H; 7.577 (7.6; 1.6) d; 1H; 7.841 (8) d; 1H; 7.995 (8) d; 1H; 8.372 (8)		−548.6
19	s; 2H; 5.094	s; 6H; 1.284			s; 2H; 3.736	d; 1H; 7.250 (9) t; 1H; 7.447 (7.6) t; 1H; 7.591 (8) t; 2H; 7.788 (7.6) d; 1H; 8.313 (8)	s; 3H; 2.668 ($CH_3C=N$)	−547.8
20	s; 2H; 5.024	s; 6H; 1.178	s; 1H; 8.860		s; 2H; 3.729	d; 1H; 5.945 (2) d; 1H; 5.976 (2)	s; 3H; 3.780 s; 3H; 3.847 (OCH_3)	−549.4

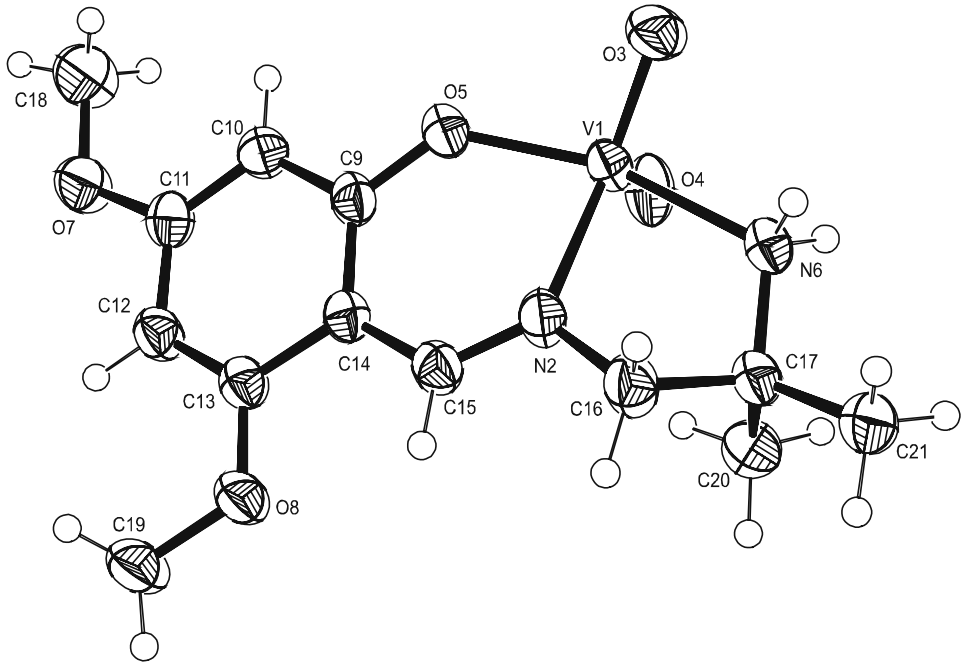

Fig. 2. An ORTEP drawing of the crystal structure of **20** with the atomic numbering scheme.

conformation, but in that case on C17. Bond lengths and angles of special interest are given in Table 2. They fall in the ranges seen in the reported TBP VO_2L complexes [13,14,20]. In contrast to the structure of reported dioxovanadium(V) complexes with Schiff base ligands comprising primary amine function [20] the crystal structure of the present monomeric complex is stabilized by the intermolecular hydrogen bonds linking the neighbouring molecules into infinite chains along the *a* axis. Hydrogen bonds between dioxovanadium oxygen atoms of a molecule and amino nitrogen atoms of neighbouring molecules result in formation of infinite –H···O=V=O···H–N–H···O= chains and closed loops, extending in the *a* direction, shown schematically in Fig. 3. These loops may be descripted as in the notation of graph-set analysis [24]. Parameters of hydrogen bonding geometry are given in Table 4.

Apart from the intermolecular hydrogen bonds there are also intra and intermolecular C–H···O and intramolecular C–H···N close contacts shown in Table 4. The C15–H15···O8 and C19–H19···O4 contacts shorter or comparable than the sum van der Waals radii for C and O may be regarded as attractive [25].

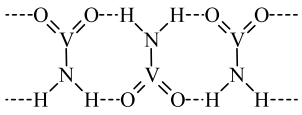

Fig. 3. The schematic representation of intermolecular hydrogen bonds in **20**. To gain higher clarity atoms of the tridentate ligand, except those of the NH_2 group, were omitted.

Table 4
Hydrogen bonding geometry and other close contacts (Å, °) for **20**

DH···A	D–H	H···A	D···A	DH···A
N6–H_N6a···O4^{i}	0.86(2)	2.04(2)	2.903(2)	173(2)
N6–H_N6b···O3^{ii}	0.86(4)	2.16(2)	3.005(2)	169(2)
C15–H15···O8	0.93(2)	2.34(2)	2.707(2)	103(2)
C19–H19···O4^{iii}	0.96(2)	2.40(3)	3.231(3)	145(3)
C20–H20a···N2	0.96(2)	2.59(2)	2.970(3)	104(2)
C21–H21b···O8^{iv}	0.96(4)	2.59(2)	3.527(3)	166(2)

Symmetry code: (i) $-x, 1-y, -z$; (ii) $1-x, 1-y, -z$; (iii) $-x, 1-y, 1-z$; (iv) $x, \frac{1}{2}-y, \frac{1}{2}-z$.

3.2. Catalytic oxidation of methyl phenyl sulfide (thioanisole)

Fig. 4(a and b) show the time dependence of the decrease in methyl phenyl sulfide and of the increase of methyl phenyl sulfoxide concentrations during the oxidation of the former compound by cumene hydroperoxide in the presence of catalytic amounts of **2** or **12**. With the cumene hydroperoxide in larger excess the oxidation of the sulfide proceeds as the reaction of first order. The plots of $\log([S]_t/[S]_o)$ versus time gave straight lines in the range of three half-lives shown in Fig. 4(c), where the [S] denote concentration of the sulfide at the subscripted time. Complexes comprising other substituents in position 5 than MeO in the salicydene part of the ligand showed no or very low catalytic activity in comparable experimental conditions. Mimoun et al. [26] pointed out the importance of sufficiently nucleophilic centre for the oxidative catalysis of organic

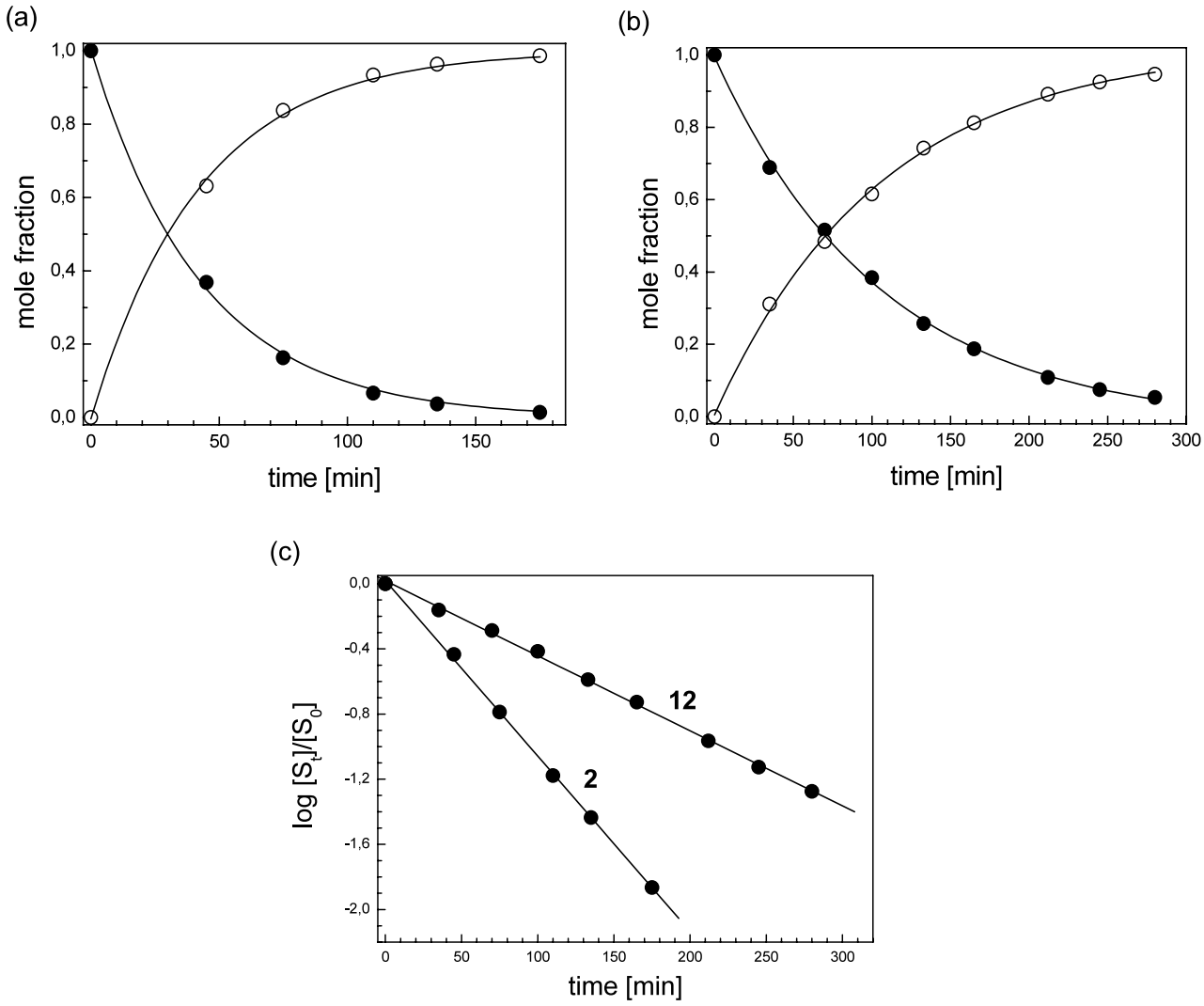

Fig. 4. Oxidation of methyl phenyl sulfide by cumene hydroperoxide with dioxovanadium(V) complexes as catalysts in DMSO at 50 °C. (a) for **2**; (b) for **12**: reaction profile: sulfide, sulfoxide; (c) plot of $\log[S_t]/[S_o]$ vs. reaction time. [S] = sulfide concentration.

substances by peroxovanadium(V) compounds. The enhanced catalytic activity of **2** and **12** as compared to other compounds may be the result of a higher electron density on the phenolato oxygen due to the electronic effects of *para*-substituted methoxy group, contributing to an attainment of sufficient nucleophility by the vanadium centre.

Slopes of lines representing the logarithm of variable concentration in relation to time (Fig. 4(c)) indicate that catalytic oxidation of the methyl phenyl sulfide proceeds significantly faster in the presence of **2** than of **12**.

4. Supplementary material

Crystallographic data for the structural analysis have been deposited with the Cambridge Crystallographic Data Centre, CCDC No. 196199 for compound 2-(4-amino-4-methyl-2-aza-1-penten-1-yl-κ^2N)-3,5-di-methoxyphenolato-κO-dioxovanadium(V). Copies of this information may be obtained free of charge from The Director, CCDC, 12 Union Road, Cambridge, CB2 1EZ, UK (fax: +44-1223-336033; e-mail: deposit@ccdc.cam.ac.uk or www: http://www.ccdc.cam.ac.uk).

Acknowledgements

The research was supported by the Grant from the Polish State Committee for Scientific Research (KBN 7 T09A 132 20).

References

[1] D. Rehder, Angew. Chem., Int. Ed. Engl. 30 (1991) 148.
[2] A. Butler, C. Carrano, Coord. Chem. Rev. 109 (1991) 61.
[3] K.H. Thompson, C. Orvig, J. Chem. Soc., Dalton Trans. (2000) 2885.

[4] R. Wever, E. De Boer, B.E. Krenn, H. Offenberg, H. Plat, Prog. Clin. Biol. Res. 274 (1988) 477.
[5] R. Wever, H. Hemrika, in: J.O. Nriagu (Ed.), Vanadium in the Environment. Part 1. Chemistry and Biochemistry, Wiley, New York, 1997, pp. 309–315.
[6] R.R. Everett, J.R. Kanovsky, A. Butler, J. Biol. Chem. 265 (1990) 4908.
[7] R.R. Everett, H.S. Soedjak, A. Butler, J. Biol. Chem. 265 (1990) 15671.
[8] H.B. den Brink, A. Tuynman, H.L. Dekker, W. Hemrika, Y. Izumi, T. Oshiro, U.E. Shoemaker, R. Wever, Inorg. Chem. 37 (1998) 6780.
[9] M. Anderson, A. Willets, S. Allenmark, J. Org. Chem. 62 (1988) 8455.
[10] M. Anderson, S.G. Allenmark, Tetrahedron 54 (1998) 15293.
[11] A. Messerschmidt, L. Prade, R. Wever, Biol. Chem. 378 (1997) 309.
[12] D. Rehder, Coord. Chem. Rev. 182 (1999) 297.
[13] L.M. Mokry, C.J. Carrano, Inorg. Chem. 32 (1993) 6119.
[14] G. Asgedom, A. Sreedhara, J. Kivikoski, E. Kolehmainen, C.P. Rao, J. Chem. Soc., Dalton Trans. (1996) 93.
[15] K. Nakajima, K. Kojima, M. Kojima, J. Fujita, Bull. Chem. Soc. Jpn. 63 (1990) 2620.
[16] C. Bolm, F. Bienewald, Angew. Chem., Int. Ed. Engl. 34 (1995) 2640.
[17] H. Schmidt, M. Bashirpoor, D. Rehder, J. Chem. Soc., Dalton Trans. (1996) 3865.
[18] G.M. Sheldrick, SHELXS-97, Program for Crystal Structure Solution,University of Göttingen, Germany.
[19] G.M. Sheldrick, SHELXL-97, Program for Crystal Structure Refinement, University of Göttingen, Germany.
[20] C.A. Root, J.D. Hoeschele, C.R. Cornman, J.W. Kampf, V.L. Pecoraro, Inorg. Chem. 82 (1993) 3855.
[21] H. Günther, NMR Spectroscopy. An Introduction, Wiley, New York, 1980, p. 87.
[22] R.R. Holmes, Prog. Inorg. Chem. 32 (1984) 119.
[23] D. Cremer, J.A. Pople, J. Am. Chem. Soc. 97 (1975) 1354.
[24] M.C. Etter, J.C. McDonald, J. Bernstein, Acta Crystallgr., Sect. B 46 (1998) 256.
[25] T. Steiner, Crystallogr. Rev. 6 (1996) 1.
[26] M. Mimoun, P. Chaumette, M. Mignard, L. Sausinne, J. Fischer, R. Weiss, Nouv. J. Chim. 7 (1983) 467.